Human Molecular Genetics, 2005, Vol. 14, No. 2 **279–293**
doi:10.1093/hmg/ddi025
Advance Access published on November 24, 2004

Dominant collagen VI mutations are a common cause of Ullrich congenital muscular dystrophy

Naomi L. Baker[1], Matthias Mörgelin[2], Rachel Peat[3], Nathalie Goemans[4], Kathryn N. North[3], John F. Bateman[1] and Shireen R. Lamandé[1,*]

[1]Cell and Matrix Biology, Murdoch Childrens Research Institute and Department of Paediatrics, University of Melbourne, Royal Children's Hospital, Parkville, Victoria 3052, Australia, [2]Department of Cell and Molecular Biology, Section of Molecular Pathogenesis, Lund University, 221 84 Lund, Sweden, [3]Institute for Neuromuscular Research, The Children's Hospital at Westmead and Department of Paediatrics and Child Health, University of Sydney, Australia and [4]Department of Paediatric Neurology, University Hospital, Leuven, Belgium

Received June 1, 2004; Revised and Accepted November 11, 2004

Mutations in the three collagen VI genes *COL6A1, COL6A2* and *COL6A3* cause Bethlem myopathy and Ullrich congenital muscular dystrophy (UCMD). UCMD, a severe disorder characterized by congenital muscle weakness, proximal joint contractures and marked distal joint hyperextensibility, has been considered a recessive condition, and homozygous or compound heterozygous mutations have been defined in *COL6A2* and *COL6A3.* In contrast, the milder disorder Bethlem myopathy shows clear dominant inheritance and is caused by heterozygous mutations in *COL6A1, COL6A2* and *COL6A3.* This model, where dominant mutations cause mild Bethlem myopathy and recessive mutations cause severe UCMD was recently challenged when a patient with UCMD was shown to have a heterozygous in-frame deletion in *COL6A1.* We have studied five patients with a clinical diagnosis of UCMD. Three patients had heterozygous in-frame deletions in the N-terminal region of the triple helical domain, one in the α1(VI) chain, one in α2(VI) and one in α3(VI). Collagen VI protein biosynthesis and assembly studies showed that these mutations act in a dominant negative fashion and result in severe collagen VI matrix deficiencies. One patient had recessive amino acid changes in the C2 subdomain of α2(VI), which prevented collagen VI assembly. No collagen VI mutations were found in the fifth patient. These data demonstrate that rather than being a rare cause of UCMD, dominant mutations are common in UCMD, now accounting for four of the 14 published cases. Mutation detection in this disorder remains critical for accurate genetic counseling of patients and their families.

INTRODUCTION

Collagen VI is a ubiquitous extracellular matrix protein that is made up of three distinct subunits, α1(VI), α2(VI) and α3(VI) (1,2). Mutations in the three collagen VI genes *COL6A1, COL6A2* and *COL6A3* cause Bethlem myopathy (MIM 158810) and Ullrich congenital muscular dystrophy (UCMD, MIM 254090) and identify collagen VI as a critical component of skeletal muscle. The collagen VI chains all have a central triple helical domain of 335–336 amino acids with repeating Gly-Xaa-Yaa sequences, and C- and N-terminal globular domains that are predominantly composed of ~200 amino acid subdomains with homology to von Willebrand factor type A domains (3–6). Intracellular collagen VI assembly is complex, initially involving association of the three chains and folding into a triple helical heterotrimeric monomer. The monomers then align in an antiparallel staggered manner to form disulfide bonded dimers that then align laterally to form tetramers, also stabilized by disulfide bonds (1,2). Tetramers are secreted and associate end-to-end to form the characteristic beaded microfibrils.

Bethlem myopathy was the first disorder to be associated with collagen VI mutations (7). It is a relatively mild dominantly inherited disorder with slow progression, characterized by early childhood onset of proximal muscle weakness and commonly, flexion contractures that mainly affect the elbows, ankles and fingers (8). The 10 distinct mutations that have been characterized in the three collagen VI genes include single amino acid substitutions (7,9–11), splice site mutations resulting in in-frame deletions (12–14) and a *COL6A1* splice

*To whom correspondence should be addressed. Tel: +61 393456650; Fax: +61 393457997; Email: shireen.lamande@mcri.edu.au

site mutation that leads to a single base deletion from the mRNA, a codon reading frameshift and the introduction of a premature stop codon (15). The effect of some of the Bethlem myopathy mutations on collagen VI biosynthesis, assembly and structure has been studied. Both the α1(VI) premature stop codon mutation and the α1(VI) exon 14 deletion result in secretion of reduced amounts of structurally normal collagen VI, either because mutant chains are not produced (15) or because they are incorporated into monomers that fail to form dimers or tetramers and are not secreted (13). In contrast, chains containing glycine substitutions towards the N-terminal region of the triple helical domain are incorporated into tetramers and microfibrils, and in these cases Bethlem myopathy results from the presence of mutant collagen VI in the extracellular matrix (16).

UCMD shows a much more severe and progressive course than Bethlem myopathy. Its hallmarks are congenital muscle weakness, proximal joint contractures and marked distal joint hyperextensibility with normal intelligence (17–20). Many patients have congenital hip dislocations and torticollis, high-arched palate, prominent heels, scoliosis and a 'sandpaper' skin rash. Motor milestones are delayed, and some patients are never able to walk independently. The respiratory muscles are also affected and some patients require night-time ventilation support by their second decade. Recessive mutations, either homozygous or compound heterozygous, in *COL6A2* and *COL6A3* have now been described in nine UCMD patients (21–25). Eight of the 11 distinct mutations lead to the introduction of premature stop codons, and in three patients with recessive *COL6A2* premature stop codon mutations, the α2(VI) mRNA undergoes nonsense-mediated mRNA decay leading to very low or no α2(VI) mRNA or protein expression (26). Nonsense-mediated mRNA decay presumably also occurs in the other UCMD patients with premature stop codon mutations although this has not yet been demonstrated experimentally. Since all three chains are required to form a collagen VI monomer, these patients are unable to assemble or secrete functional collagen VI protein and collagen VI is almost absent from muscle and fibroblasts (21). The other three recessive UCMD mutations are in-frame deletions (22,25). Their effect on collagen VI biosynthesis and assembly has not been studied in detail.

This model, where dominant collagen VI mutations cause mild Bethlem myopathy and recessive mutations cause the more severe disorder UCMD, was recently challenged when a patient with severe UCMD was shown to have a heterozygous in-frame deletion in the *COL6A1* gene (27). No other collagen VI mutations were found. The genomic deletion was not present in either parent indicating that it was a *de novo* mutation in the patient. Protein biosynthetic studies provided critical insights into the consequences of this mutation that explain how a severe UCMD phenotype can result from a heterozygous mutation. Mutant α1(VI) chains, with a 33 amino acid deletion towards the N-terminal region of the triple helical domain, were able to assemble with normal α2(VI) and α3(VI) to form monomers, then dimers and tetramers, and some mutant-containing tetramers were secreted. The stoichiometry of the multistep collagen VI intracellular assembly process means that only 1/16 of the tetramers produced by this patient could be composed entirely of normal chains. Collagen VI was almost completely absent from the fibroblast matrix, indicating that the effect of the mutation was further amplified in the microfibril assembly step where the tetramers join end-to-end via their N-terminal regions. Thus, in this case, UCMD resulted from a heterozygous mutation that exerted a dominant negative effect on collagen VI structure and assembly.

In this study, we have examined a group of five patients with a clinical diagnosis of UCMD. Surprisingly, three patients had dominant heterozygous in-frame deletions in the N-terminal region of the triple helical domain. Detailed collagen VI protein biosynthesis and assembly studies showed that these mutations act in a dominant negative fashion and result in severe collagen VI matrix deficiencies. One patient had recessive amino acid changes in the C-terminal C2 subdomain of the α2(VI) chain, which prevented assembly of collagen VI monomers. No collagen VI mutations were found in the fifth patient. These data indicate that dominant mutations are a common cause of UCMD and emphasize the importance of mutation detection for accurate genetic counseling for patients and their families.

RESULTS

Five patients with UCMD

The five patients included in this study, UCMD1, 2, 3, 4 and 5, all presented with the signature clinical features of UCMD, including congenital muscle weakness, proximal joint contractures and marked distal joint hyperextensibility. UCMD1, 2, 4 and 5 have a striking similarity in their facial appearance. They have a round face, small chin and lips, irregular crowded teeth, large round eyes and prominent ears. In contrast, UCMD3 has small eyes and obvious facial muscle weakness. All five patients show signs of skin abnormalities. UCMD1, 2, 3 and 4 have abnormal scarring, UCMD2 and 4 have mild hyperkeratosis of the upper arms and UCMD5 has a reddish papular rash over the face and arms.

In addition to these features, UCMD1, the first child of healthy unrelated parents, had congenital bilateral hip dislocation, scoliosis and torticollis. Clinical evaluation at 6 months of age showed severe hyperlaxity and muscle atrophy. Creatine kinase levels were normal and electromyography (EMG) showed a myogenic pattern. An MRI scan at 5 years showed no brain abnormalities and cardiac function was also normal. This patient was able to sit at 11 months, and walked at 21 months. She required night-time ventilation assistance from age 7. At age 8, she was extremely dystrophic, with growth delay despite gastrostomy feeding, was able to walk independently for short distances but unable to climb stairs. She had severe hyperlaxity of the fingers, contractures of the hips, knees, elbows and ankles and severe progressive scoliosis.

UCMD2 is now 11 years old and the only child of healthy non-consanguineous parents. She presented with congenital hypotonia, proximal joint contractures, distal joint hyperextensibility, scoliosis, torticollis and bilateral hip dislocations. She was able to sit at 13 months, crawl at 15 months and walk at 17 months, although she lost independent ambulation at 10 years. Creatine kinase levels were normal, and a muscle biopsy at age 8 showed a dystrophic pattern with an increase

in endomysial fibrosis and an increased number of internal nuclei. She has hip, knee, elbow and ankle contractures, marked hyperlaxity of the fingers, a progressive scoliosis and a severe decline in respiratory function, with vital capacity $<40\%$.

UCMD3, the second child of healthy unrelated parents, is currently 12 years old and presented at birth with the typical clinical features of UCMD including muscle weakness, hip contractures and distal hyperlaxity. She was able to sit at 7 months and walk at 18 months with a waddling, unsteady gait. A muscle biopsy at 3 years showed variation in fiber size and increased endomysial fibrosis. Creatine kinase was normal. She developed early and progressive retractions of the Achilles tendons and has twice had surgery to release the contractures. At 7 years she was severely dystrophic with striking muscle hypotonia, marked hyperlaxity of the fingers, scoliosis and contractures of the ankles and hips. She has difficulty closing her mouth and feeding and has restricted respiratory function. Her intellectual development is normal.

UCMD4, the first and only child of healthy unrelated parents, presented at birth with hypotonia, joint laxity and hip dislocation. He was able to sit at 11 months and walk independently at 3 years, but lost ambulation at 4 years of age. Progressive joint contractures were present from age 2. Currently 19 years old, he has severe joint contractures, severe muscle wasting, scoliosis, torticollis, striking hyperlaxity of the fingers and is severely dystrophic, despite gastrostomy feeding. He required nocturnal ventilation from 7 years of age and currently also receives ventilation during part of the day. An EMG at age 3 showed a myogenic pattern, and muscle biopsy demonstrated a severe increase of fibrosis, variation in fiber size and small clusters of atrophic fibers. Creatine kinase was normal, and there was no heart involvement. Brain MRI was normal.

UCMD5 is the third child born to unrelated parents, and there is no history of neuromuscular disease. He presented in the neonatal period with subluxated and dysplastic hips, contractures at the ankles, knees and elbows, hyperextensible fingers and a fracture of the distal femoral epiphysis, likely sustained during delivery. He crawled independently at 16 months of age and walked with assistance by 2 years of age. He has normal cognitive development. Creatine kinase, echocardiography, respiratory function and EMG have remained normal. Muscle biopsy performed at 2 years of age demonstrated variability in fiber size, increased interstitial connective tissue and scattered regenerating fibers consistent with a mild dystrophic pathology. Currently 12 years of age, he has generalized poor muscle bulk and generalized muscle weakness, more marked proximally. He has a high palate, cervical kyphosis, a mild thoracic scoliosis, hyperextensible wrists and long tapering fingers, and very prominent heels.

UCMD patient fibroblasts produce normal levels of collagen VI mRNAs

Eight of the 11 recessive mutations that have been characterized in UCMD patients lead to the introduction of premature stop codons in the α2(VI) and α3(VI) mRNAs (21–25). The most common consequence of premature termination mutations in many genes is rapid degradation of the mutant mRNA by a process known as nonsense-mediated mRNA decay (28,29), and this is also the case for collagen VI. The three α2(VI) UCMD premature stop codon mutations that have been examined result in either the complete absence or a severe reduction in the level of the affected mRNA seen on northern blots (26). Nonsense-mediated mRNA decay was also seen in a Bethlem myopathy patient with a heterozygous α1(VI) premature stop mutation (15). To determine whether our UCMD patients had mutations that resulted in mRNA degradation, total RNA from fibroblasts was separated on a denaturing agarose gel, transferred to nitrocellulose, and hybridized simultaneously to radiolabeled α1(VI), α2(VI) and α3(VI) cDNAs. All three collagen VI mRNAs were present in these patients, and their relative expression levels were similar to that of the control (Fig. 1), indicating that unlike the majority of UCMD cases reported to date, these patients do not have premature stop codon mutations leading to mRNA decay or mutations that prevent transcription of one of the genes.

UCMD1, 2, 4 and 5 have a collagen VI deficiency

To confirm that a collagen VI protein deficiency was the underlying cause of the UCMD phenotype in these five patients, we examined the accumulation of collagen VI microfibrils in the fibroblast extracellular matrix. Confluent cultures were incubated for 2 days in the presence of sodium ascorbate to promote deposition of a collagenous extracellular matrix, then stained prior to fixation with a specific collagen VI antibody. This ensured that only extracellular collagen VI was detected. Collagen VI was almost completely absent from the UCMD2 extracellular matrix, and when compared with controls, UCMD1, 4, and 5 matrices contained significantly less collagen VI (Fig. 2A). Collagen VI staining in the UCMD3 fibroblast matrix was not significantly different to the controls. To determine whether collagen VI synthesis and secretion were altered in these patients, the amount of collagen VI in the fibroblast culture medium was compared by immunoblotting. Collagen VI tetramers were not detected in UCMD2 culture medium, UCMD1, 4 and 5 secreted reduced amounts of collagen VI and UCMD3 produced similar amounts of collagen VI to controls (Fig. 2B). Together, these data confirmed that at least four of the five patients, UCMD1, 2, 4 and 5, had collagen VI abnormalities.

Immunostaining of a muscle biopsy from UCMD5 with perlecan and collagen VI antibodies demonstrated that the collagen VI was abnormally localized in this patient (Fig 2C). In normal muscle, the collagen VI co-localized with perlecan in the basement membranes surrounding the muscle fibers. Collagen VI was also present in the interstitial extracellular matrix between fibers in control muscle. However, in UCMD5 collagen VI was not concentrated in the basement membranes, but was present in the interstitial extracellular matrix between individual muscle fibers and surrounding fiber bundles (Fig. 2C). This is consistent with the observed reduction in collagen VI specifically at the basement membrane, which has been reported in other UCMD patients (22,27).

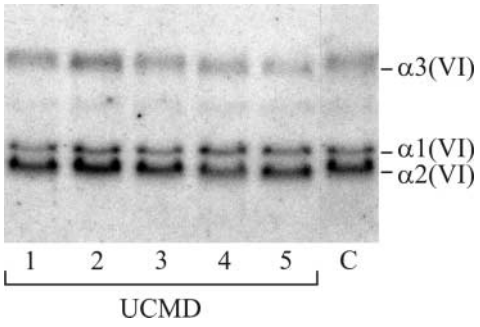

Figure 1. Expression of α1(VI), α2(VI) and α3(VI) mRNAs in UCMD fibroblasts. Total RNA (5 μg) isolated from control (*C*) and UCMD1, 2, 3, 4 and 5 fibroblasts was separated on a denaturing agarose gel, transferred to nitrocellulose and hybridized simultaneously to [α-^{32}P]dCTP-labeled α1(VI), α2(VI) and α3(VI) cDNA probes. The migration positions of the α1(VI), α2(VI) and α3(VI) mRNAs are indicated. The three collagen VI mRNAs were present in the patients and the relative expression levels were similar to the control.

Abnormal collagen VI intracellular assembly in UCMD1, 2, 4 and 5

The finding that UCMD1, 2, 4 and 5 fibroblasts had normal amounts of α1(VI), α2(VI) and α3(VI) mRNAs but reduced extracellular collagen VI, suggested that underlying structural mutations affect the assembly and secretion of collagen VI tetramers. To examine collagen VI biosynthesis and assembly, confluent fibroblast cultures were labeled overnight with ^{35}S-methionine and the collagen VI in the cell and medium fractions was immunoprecipitated with an antibody made to the recombinant α3(VI) N1 subdomain. The individual collagen VI chains were resolved on 3–8% gradient polyacrylamide gels under reducing conditions (Fig. 3A). In UCMD2, α3(VI) chains were immunoprecipitated from the cell fraction; however, co-immunoprecipitated α1(VI) and α2(VI) chains were barely detectable (Fig. 3A, lane 4), suggesting that the mutations in this patient affected the ability of the mutant chains to assemble with normal chains to form a triple helical collagen VI monomer. Consistent with this, only minute amounts of collagen VI were immunoprecipitated from UCMD2 medium (Fig. 3A and B, lane 11). In addition to the normal α1(VI) and α2(VI) chains, the UCMD1 cell sample, contained a faster migrating band (Fig. 3A, lane 3), suggesting that either the α1(VI) or α2(VI) chain contained a deletion. In the UCMD4 cell sample, the relative intensities of the α1(VI) and α2(VI) bands were reversed (Fig. 3A, lane 6), suggesting an underlying deletion in the α2(VI) chain which normally migrates more slowly than the α1(VI) chain (26). In both patients, co-immunoprecipitation of the mutant chains with the α3(VI) antibody indicated that they were able to associate with normal chains. No migration differences of the individual chains were obvious in UCMD3 or 5 samples.

The ability of the UCMD collagen VI to assemble into dimers and tetramers was assessed by analysis of the immunoprecipitated collagen VI on non-reducing composite agarose/acrylamide gels. In both control and UCMD cultures, tetramers were the predominant secreted form of collagen VI (Fig. 3B). However, UCMD1, 4 and 5 cells showed intracellular collagen VI assemblies that migrated with a molecular mass consistent with a collagen VI dimer (~1000 kDa, Fig. 3B, lanes 3, 6 and 7). This indicated that the mutations in these three patients did not affect the assembly of collagen VI into monomers or dimers, but interfered with the association of dimers to form disulfide bonded tetramers. Dimers were also apparent in the medium of UCMD1, 4 and 5 (Fig. 3B, lanes 10, 13 and 14), indicating that some of the collagen VI secreted by these patients is structurally abnormal and probably contains mutant chains. No differences in collagen VI biosynthesis and assembly could be detected in UCMD3 (Fig. 3A and B).

Microfibril assembly defects in UCMD1, 4 and 5

Following secretion, collagen VI tetramers associate end-to-end to form long thin microfibrils. To visualize the collagen VI tetramers that were secreted by the UCMD fibroblasts, medium from control and UCMD cultures was examined by negative staining electron microscopy. Microfibril formation was then quantified by analysis of a large number of micrograph fields (Fig. 4A). The occurrence of 'microfibrils' containing 1–10 tetramers is shown as a percentage of the total number of microfibrils. Though tetramers were seen in the medium from UCMD2 cultures, they were extremely rare and microfibril formation was not quantitated. In control fibroblasts, ~20% of the microfibrils were single tetramers and microfibrils containing up to 10 tetramers were seen (Fig. 4A). In contrast, medium from UCMD1, 4 and 5 cells contained a larger proportion of single tetramers, accounting for 40–60% of the 'microfibrils', and microfibrils containing more than six tetramers were not seen (Fig. 4A). This indicated that the mutations in these three patients led to a reduction in the efficiency of end-to-end assembly of tetramers, and suggested that tetramers containing mutant chains were secreted.

A striking finding was that some of the UCMD3 collagen VI microfibrils had formed unusual large aggregates (Fig. 4B). These kinds of aggregates were not seen in control medium where only individual microfibrils were observed (Fig. 4B) or in the medium from the other UCMD cultures. This finding suggested that the collagen VI from UCMD3 was structurally abnormal even though no other biosynthetic or assembly abnormalities had been found. Not all of the UCMD3 collagen VI had formed aggregates, and when UCMD3 microfibril formation was quantified using fields with individual non-aggregated microfibrils, it was similar to the controls (Fig. 4A).

UCMD1, 4 and 5 have dominant heterozygous deletions in the collagen VI triple helical domain

The mutations in UCMD1, 4 and 5 were localized using RT–PCR to amplify α1(VI), α2(VI) and α3(VI) mRNAs. In UCMD1, an RT–PCR product corresponding to exons 7–15 of the *COL6A1* gene contained a band of the expected size and a smaller mutant band (Fig. 5A). The normal and mutant products were of similar intensity confirming that the mutant mRNA was stable. Direct sequencing of the two RT–PCR products demonstrated that the smaller product lacked the 27 nucleotides encoded by *COL6A1* exon 12

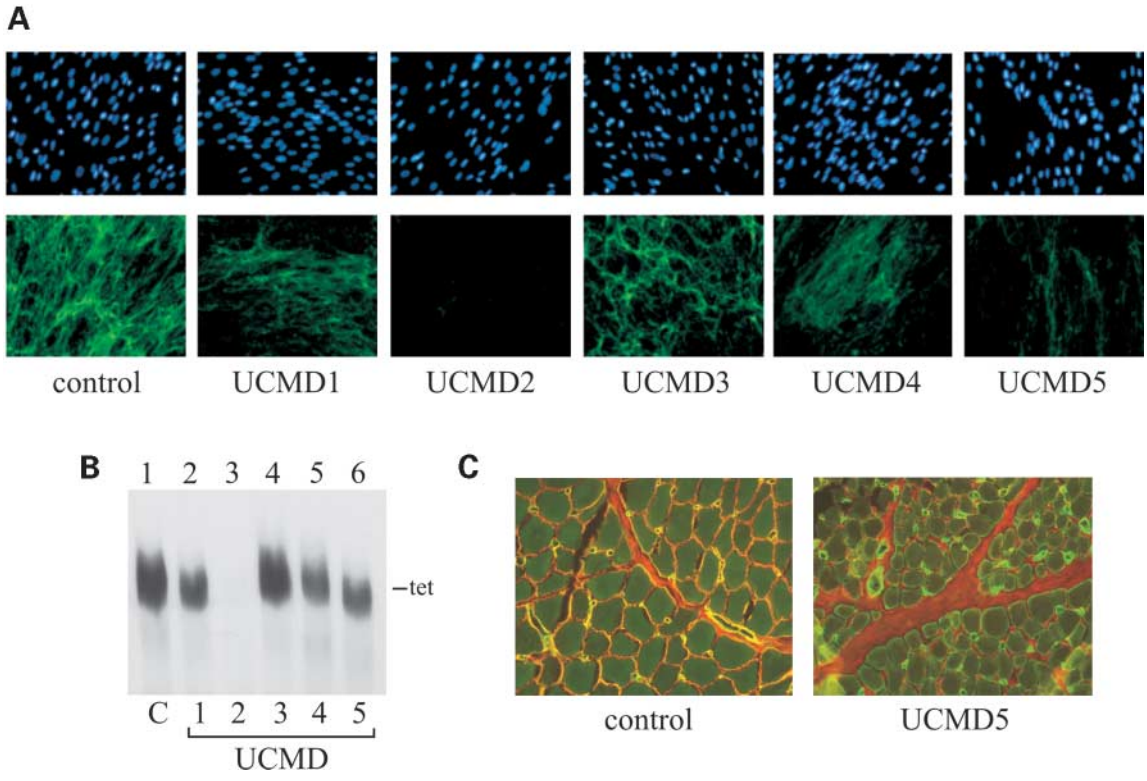

Figure 2. UCMD1, 2, 4 and 5 have a collagen VI deficiency. **(A)** Control and UCMD fibroblasts were grown for 2 days post-confluency in the presence of sodium ascorbate to promote deposition of a collagenous extracellular matrix, then stained prior to fixation with a collagen VI antibody (lower panels). Cell nuclei were stained with DAPI (upper panels). Collagen VI was absent from the UCMD2 extracellular matrix, and when compared with controls, UCMD1, 4 and 5 matrices contained significantly less collagen VI. The UCMD3 collagen VI matrix was similar to controls. Images are 20×. **(B)** Control (*C*, lane 1) and UCMD fibroblasts (lanes 2–6) were incubated overnight in serum-free medium, then equal aliquots of the medium were separated on a non-reducing composite gel. Proteins were transferred to a nylon membrane and collagen VI detected with a specific antibody. Collagen VI tetramers are indicated on the right. UCMD3 (lane 4) secreted similar amounts of collagen VI as the control, collagen VI was not detected in the medium of UCMD2 (lane 3) and UCMD1, 4 and 5 (lanes 2, 5 and 6) all secreted reduced amounts of collagen VI tetramers. **(C)** Muscle biopsies from control and UCMD5 were stained with collagen VI (red fluorescence) and perlecan (green fluorescence) antibodies and the images were overlayed. In control muscle, collagen VI and perlecan co-localize in the basement membrane (yellow). In UCMD5 muscle, collagen VI is not co-localized in the basement membrane with perlecan and is predominantly localized in the interstitial matrix between individual muscle fibers. Images are 40×.

(data not shown). This nine amino acid deletion, residues 311–319 (amino acids 55–63 of the triple helical domain), maintained the normal reading frame and was consistent with the protein analysis that had detected a faster migrating α1(VI) or α2(VI) chain (Fig. 3A). Exon skipping is most often the result of a consensus splice site mutation, and so genomic DNA from the patient was PCR amplified and directly sequenced. A heterozygous IVS12+1 g>a mutation in the obligatory splice site was identified (Fig. 5B). All but one of the UCMD cases that have been characterized to date have a recessively inherited disorder and either homozygous or compound heterozygous mutations inherited from their unaffected heterozygous parents. However, in this case neither unaffected parent carried the mutation indicating that this was a *de novo* change in the child (Fig. 5B). We searched for a second heterozygous mutation by sequencing the entire coding regions of the α1(VI), α2(VI) and α3(VI) mRNAs but failed to find one. Four single nucleotide changes that resulted in amino acid substitutions were detected (Table 1) as well as eight silent nucleotide changes (data not shown). The silent changes were considered non-pathogenic polymorphisms for two reasons. Firstly, they were all found in controls. Secondly, the mutation analysis was based on mRNA amplification, and with the exception of the fragment containing *COL6A1* exon 12, only a single RT–PCR product was obtained for each primer set. This means that we can be sure that the silent changes did not alter mRNA splicing as has been observed in many genes (30). The amino acid substitutions were all found in both the heterozgyous and homozygous state in control genomic DNA and could also be excluded as pathogenic mutations. Together, these data demonstrate that the UCMD phenotype in this patient results from a single dominant *de novo COL6A1* mutation.

Similarly, in UCMD4 an α2(VI) RT–PCR produced a band of the expected size as well as a smaller band of equal intensity (Fig. 5C). Sequencing of the smaller band indicated that it lacked the 54 nucleotides encoded by *COL6A2* exon 6 as well as the 27 most 5′ nucleotides of exon 7 (data not shown). This mutation also maintained the normal reading frame and predicted the synthesis of a mutant α2(VI) chain with a 27 amino acid deletion: residues 268–294 (amino acids 13–39 of the triple helix). To characterize the underlying mutation

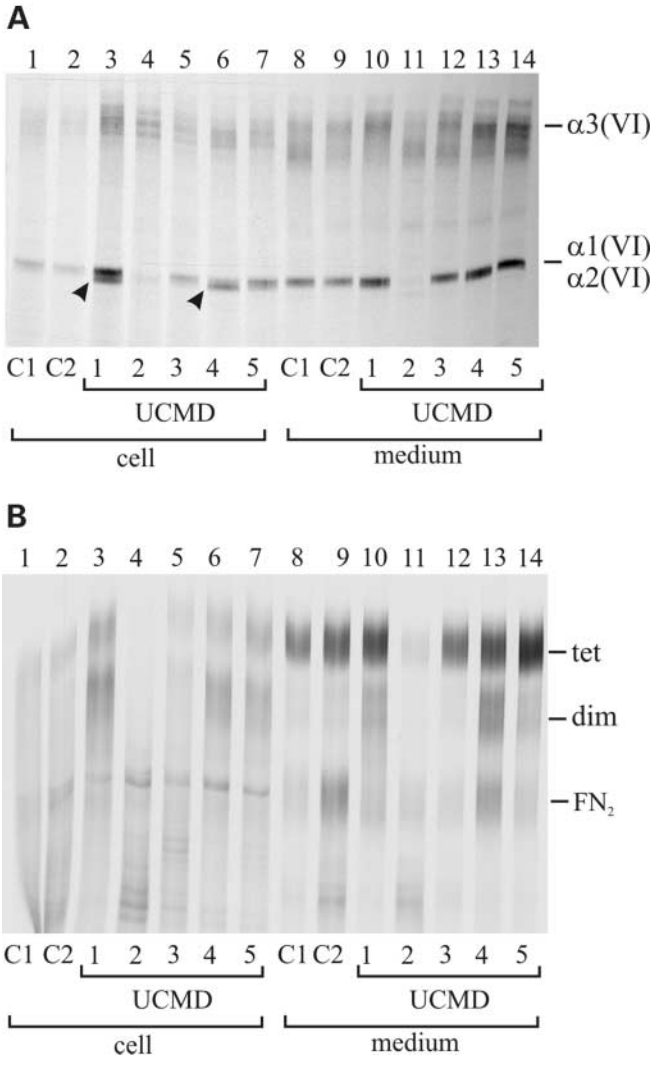

Figure 3. Electrophoretic analysis of collagen VI produced by UCMD fibroblasts. Control (*C1* and *C2*) and UCMD fibroblasts were biosynthetically labeled overnight with [^{35}S]methionine and the collagen VI in the cell and medium fractions was immunoprecipitated with an α3(VI) chain antibody. **(A)** Samples were analyzed under reducing conditions on a 3–8% gradient polyacrylamide gel. The migration positions of the individual collagen VI subunits α1(VI), α2(VI) and α3(VI) are indicated on the right. UCMD1 and 4 cell fractions contained abnormally migrating α1(VI) or α2(VI) chains (arrowheads, lanes 3 and 6) suggesting that one of these chains contained a deletion. **(B)** Samples analyzed without reduction on a composite 0.5% agarose and 2.5% acrylamide gel. Collagen VI disulfide bonded tetramers and dimers, and contaminating fibronectin dimers (FN_2) are indicated on the *right.* Only minute amounts of collagen VI were immunoprecipitated in UCMD2 (lanes 4 and 11). Collagen VI dimers were present in the cell fraction of UCMD1, 4 and 5 (lanes 3, 6 and 7) and were also seen in the medium (lanes 10, 13 and 14), indicating that some structurally normal collagen VI was secreted. No abnormalities were observed in UCMD3 fibroblasts.

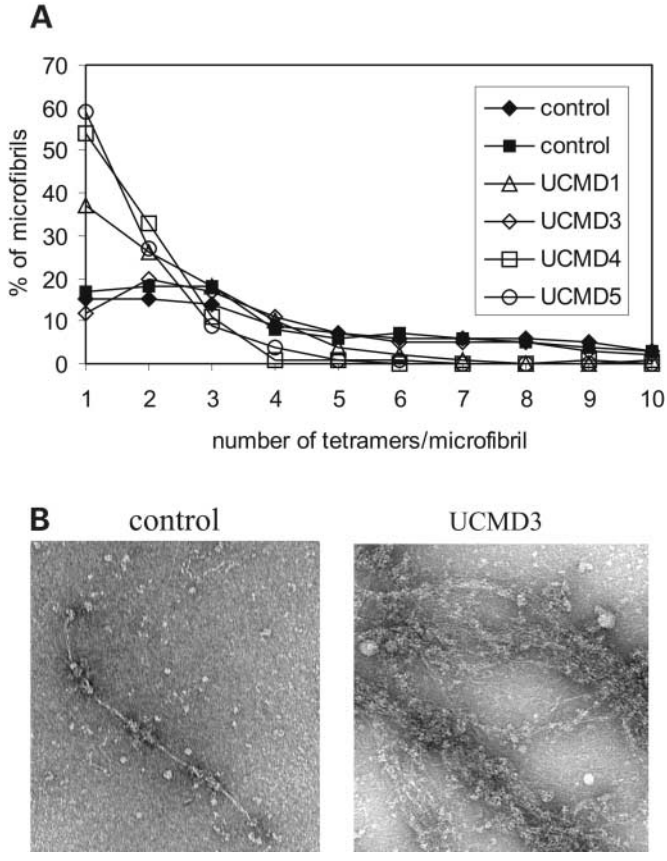

Figure 4. Quantitative analysis of collagen VI tetramer–tetramer association. Collagen VI secreted into the medium of control and UCMD fibroblasts was visualized by negative staining electron microscopy. **(A)** The ability of the tetramers to associate end-to-end was quantitated. The occurrence of microfibrils containing 1–10 tetramers is shown as a percentage of the total number of microfibrils. UCMD1, 4 and 5 medium contained a larger proportion of individual tetramers than the medium from control cells and microfibrils containing more than six tetramers were not seen, indicating that the mutations in these patients compromise collagen VI microfibril formation. UCMD3 microfibril formation was similar to control. **(B)** The medium from UCMD3 cultures contained collagen VI microfibrils that had formed unusual large aggregates. Control medium and medium from the other UCMD cultures contained only single, non-aggregated microfibrils.

in this patient, genomic DNA was amplified using a primer located within *COL6A2* intron 4 and a primer spanning the exon 8/intron 8 boundary. Under optimal conditions this primer set should amplify a band of 2488 bp. This band was not amplified in either control or UCMD4 PCRs presumably because of its large size. However, in UCMD4 a 1156 bp product that was not seen in control PCRs was amplified. Direct sequencing revealed that this product contained a 1332 bp deletion including the most 3′ 1169 bases of intron 5, all of exon 6 and intron 6, and the most 5′ 27 bases of exon 7 (Fig. 5D). The deletion juxtaposed intron 5 and exon 7 sequences and created a 3′ AG splice site motif at the junction (Fig. 5D). Comparison of the mRNA and genomic deletions demonstrated that the remaining 18 bp of exon 7 functioned as an exon and indicated that the novel splice site generated by the deletion was recognized by the pre-mRNA splicing machinery. The strength of this new 3′ splice site sequence was estimated using maximum entropy scoring software that is based on large data sets of human splice sites (31,32). The ideal MaxENT score for a 3′ splice site is 13.59 and theoretically, the larger the MaxENT value, the more efficient the splicing (31,32). The normal 3′ splice site of *COL6A2* intron 6 has a score of 10.68; however, the novel splice site generated by the deletion has a MaxENT

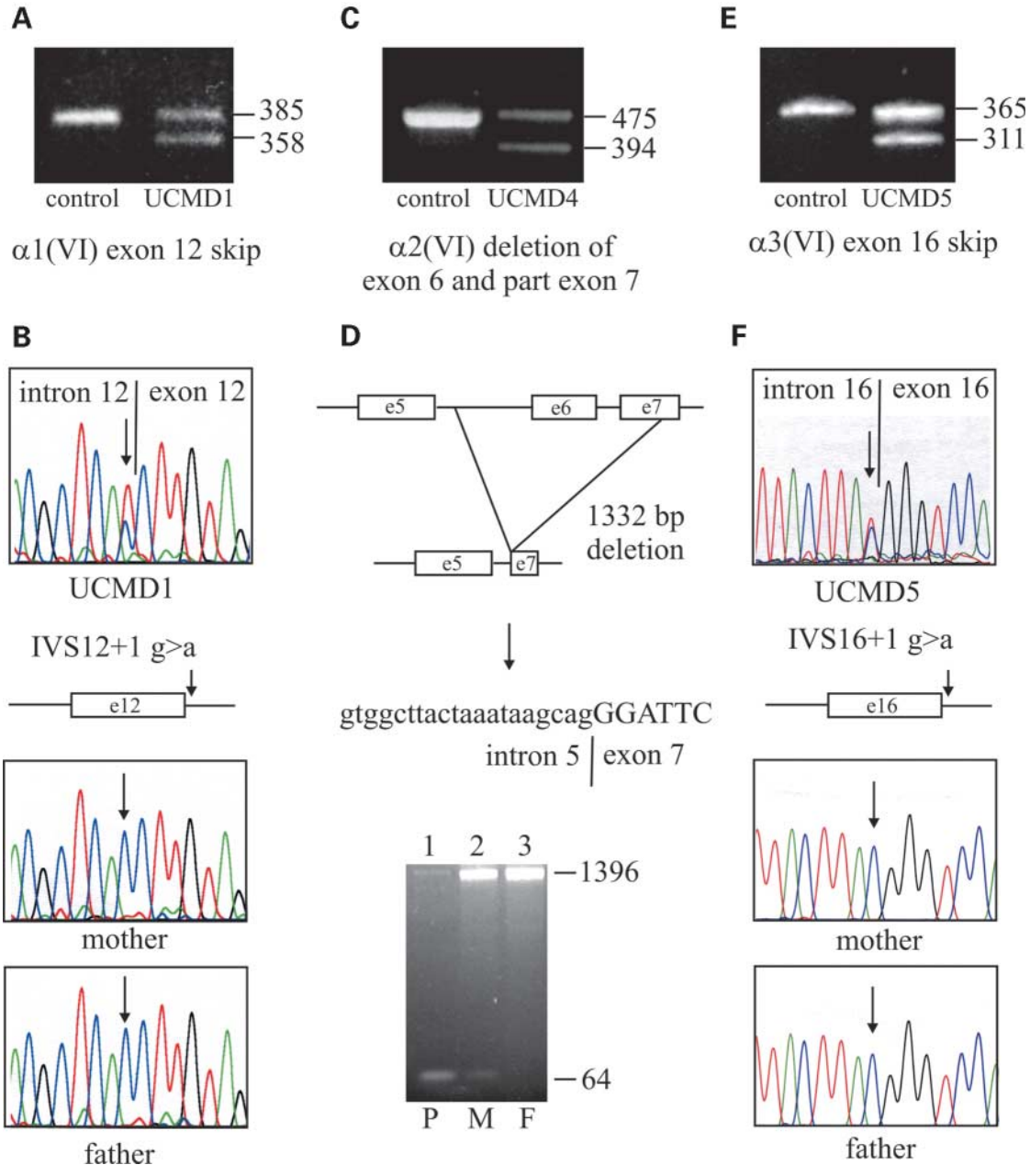

Figure 5. Heterozygous mutations in UCMD1, 4 and 5. **(A)** RT–PCR of α1(VI) bases 737–1121 showing the normal 385 bp product and the 358 bp product amplified from UCMD1 mRNA. Direct sequencing demonstrated that the smaller product lacks the bases encoded by *COL6A1* exon 12. **(B)** Genomic DNA from UCMD1 and the parents was PCR amplified using primers within introns 10 and 13 and directly sequenced. UCMD1 has a heterozygous IVS12 + 1g>a mutation that explains the exon 12 skipping. Neither parent carries the change indicating that it is a *de novo* mutation in the patient. **(C)** RT–PCR of α2(VI) bases 711–1185. UCMD4 has the normal 475 bp band and a smaller 394 bp band. Direct sequencing of the smaller band demonstrated that it lacked the 54 nucleotides encoded by *COL6A2* exon 6 and the 27 most 5′ nucleotides of exon 7. **(D)** The mutation in UCMD4 is a heterozygous 1332 bp genomic deletion that includes the most 3′ 1169 bases of intron 5, all of exon 6 and intron 6 and the most 5′ 27 bases of exon 7. The new intron 5 3′ splice site generated by the deletion is shown below the schematic. To determine whether the parents of UCMD4 carried the mutation, genomic DNA was PCR amplified using a primer located in intron 5 and a primer that spanned the exon 7/intron 7 boundary. The PCR products were resolved on an agarose gel. Both the normal 1396 bp band and the 64 bp smaller mutant product were amplified from UCMD4 DNA (*P*, lane 1). Only the normal 1396 bp band was amplified from the father's DNA (*F*, lane 3), however a small amount of the mutant 64 bp band was amplified from the mother's DNA (*M*, lane 2). The major amplified product from the mother's DNA was the 1396 bp normal band indicating that, unlike UCMD4, she was not heterozygous for the mutation but was a mosaic carrier. **(E)** RT–PCR of α3(VI) bases 6078–6442. UCMD5 has the normal 365 bp band and a smaller 311 bp band that lacks the sequences encoded by *COL6A3* exon 16. **(F)** The underlying mutation was characterized by PCR amplifying genomic DNA from UCMD5 and the parents using primers within COL6A3 introns 15 and 16 and directly sequencing the products. UCMD5 has a heterozygous IVS16 + 1g>a mutation that explains the exon skipping. Neither unaffected parent carries the mutation indicating that it is a *de novo* change in the child.

Table 1. Collagen VI amino acid changes

Exon, domain[a]	Nucleotide change	Amino acid change[b]	Status					Reference[c]
			UCMD1	UCMD2	UCMD3	UCMD4	UCMD5	
COL6A1								
35, C2	c.2549 G>A	R850H	Homo	Hetero		Hetero	Hetero	
35, C2	c.2669 C>T	S890L		Hetero				27
COL6A2								
3, N1	c.679 A>G	N227D	Homo	Homo	Homo	Homo	Homo	
14, helix	c.1196 A>G	N399S			Hetero	Hetero		
26, C1	c.2039 A>G	H680R	Hetero		Homo	Hetero	Hetero	27
28, C2	**c.2510 T>C**	**L837P**		**Hetero**				
28, C2	**c.2688delAAC**	**del N897**		**Hetero**				
COL6A3								
2, SP	c.14 G>A	R5Q				Hetero		
5, N8	c.1471 G>C	D491H			Hetero			
5, N8	c.1475 C>G	T492S			Hetero			
6, N7	c.2419 G>A	A807T		Hetero				*
6, N7	c.2488 G>T	A830S		Hetero				*
8, N5	c.3262 A>C	K1088Q		Hetero				*
10, N3	c.4727 G>A	R1576Q					Hetero	
36, C1	c.7292 T>A	V2431D	Homo	Homo	Homo	Homo	Homo	27
39, C2	c.8491 G>C	D2831H			Hetero			10
40, C3	c.8780 C>T	T2927M		Hetero	Hetero			27
40, C3	c.8870insTGC	2957insA		Homo	Hetero	Homo	Homo	10
40, C3	c.8959 G>A	V2987M		Homo	Hetero	Homo	Homo	27
41, C4	c.9031 C>G	P3011A		Hetero				
41, C4	c.9203 C>T	T3068I				Homo	Homo	27

[a]SP = signal peptide.
[b]UCMD2 changes in bold are recessive pathogenic mutations.
[c]*=A. Lampe and K. Bushby, personal communication.

score of only 0.97 and would not have been predicted to function as a splice site in the absence of the mRNA expression data.

To determine whether the unaffected parents of UCMD4 carried the deletion, genomic DNA was PCR amplified using a primer within *COL6A2* intron 5 and a primer that spanned the exon 7/intron 7 boundary. This primer set was predicted to amplify a 1396 bp band from the normal allele and a 64 bp band from the mutant allele. As expected, both bands were amplified from UCMD4 genomic DNA although the larger band was relatively faint due to differences in the amplification efficiencies of the mutant and normal alleles (Fig. 5D). Only the 1396 bp normal band was amplified from the father's DNA; however, in addition to the normal product, a small amount of the 64 bp mutant band was amplified from the mothers DNA (Fig. 5D). The relative intensities of the two bands from UCMD4 and the mother were very different. In contrast to UCMD4, the major amplified product from the mother's DNA was the 1396 bp band from the normal allele, indicating that the normal allele was much more abundant than the mutant and that the mother was not heterozygous for the mutation. This finding was reproduced in multiple PCRs and suggested that despite being phenotypically normal, the mother of UCMD4 was a mosaic carrier of the deletion. To confirm that this was the only mutation in UCMD4, the entire coding regions of the three collagen VI mRNAs were sequenced. Nine silent nucleotide changes (data not shown) and nine changes that resulted in amino acid substitutions were detected (Table 1). Eight of the amino acid substitutions were found in controls and could be considered non-pathogenic; however, we did not find the α3(VI) R5Q substitution in 108 control chromosomes. This substitution is within the signal peptide and importantly, both sequences are predicted to function as signal peptides with a probability of 1.0 (SignalP 3.0). The ability of the alternative sequences to function as signal peptides was tested experimentally in *in vitro* coupled transcription and translation reactions performed in the presence of canine microsomal membranes. Both the normal and alternative signal peptides were able to direct translocation into the microsomal membranes and both signal peptides were cleaved (data not shown), providing strong evidence that that the R5Q substitution is a rare non-pathogenic polymorphism and does not contribute to the disease phenotype in this patient.

In UCMD5, an α3(VI) RT–PCR produced a band of the expected size as well as a smaller band (Fig. 5E) that lacked the 54 bases encoded by *COL6A3* exon 16 (data not shown). This exon codes for residues 2058–2070 of the α3(VI) chain (amino acids 16–33 of the triple helix). When genomic DNA from the patient was PCR amplified and directly sequenced, a heterozygous IVS16+1 g>a mutation was identified in the obligatory 5′ consensus splice site of intron 16 (Fig. 5F) that accounts for the observed exon skipping. Importantly, the mutation was not present in either of the unaffected parents (Fig. 5F), indicating that it was a *de novo* mutation in the patient. Sequencing of the coding regions of the three collagen VI mRNAs identified 17 silent

nucleotide changes (data not shown) and eight changes that resulted in amino acid substitutions (Table 1). All of these changes were found in controls.

UCMD1, 4 and 5 thus have dominant heterozygous in-frame deletions in the triple helical domain of collagen VI. Although the mutations are in different chains, α1(VI) in UCMD1, α2(VI) in UCMD4 and α3(VI) in UCMD5, they are all located towards the N-terminal end of the triple helix, between amino acids 13 and 63 of the 335–336 residue triple helical domain.

Recessive *COL6A2* mutations in UCMD2

The finding that only a minute amount of collagen VI was assembled and secreted by UCMD2 fibroblasts suggested that this patient had homozygous or compound heterozygous structural mutations in one of the collagen chains that prevented chain association. To characterize the mutations, the entire coding regions of the α1(VI), α2(VI) and α3(VI) mRNAs were amplified by RT–PCR and directly sequenced. Sixteen silent nucleotide changes were detected (data not shown) and excluded as the pathogenic mutations as they were all found in controls. In addition, there were 13 changes that resulted in amino acid substitutions (Table 1). Five of these, α1(VI) S890L, α3(VI) V2431D, T2927M, 2957insA and V2987M, have been previously reported as polymorphisms (10,27), and three, α1(VI) R850H, α2(VI) N227D, and α3(VI) P3011A, were commonly seen in controls. We did not find the remaining five changes in 108 control chromosomes. UCMD2 inherited α3(VI) A807T, A830S and K1088Q from her unaffected father who is also heterozygous for these changes (data not shown). They have also been found in a patient with a dominantly inherited muscular dystrophy where linkage to *COL6A3* has been excluded (A. Lampe and K. Bushby, personal communication). These three changes are thus likely to be rare non-pathogenic polymorphisms. The two remaining changes, c.2510T>C (L837P) and c.2699delAAC (delN897), are both within the C2 subdomain of the α2(VI) chain and are likely to be the disease causing mutations in this patient. Consistent with this proposal, UCMD2 inherited the L837P mutation from her unaffected mother (Fig. 6A) and the N897 deletion from her unaffected father (Fig. 6B).

No detectable collagen VI or biglycan mutations in UCMD3

UCMD3 had normal levels of the three collagen VI mRNAs and no intracellular assembly or secretion defects were detected. However, the large collagen VI aggregates that were seen in the culture medium by electron microscopy suggested that there was an underlying collagen VI abnormality and so the entire coding regions of the α1(VI), α2(VI) and α3(VI) mRNAs were sequenced. No mutations were found in this patient. Thirteen non-pathogenic silent polymorphisms were present (data not shown), as well as 10 changes that resulted in amino acid substitutions (Table 1). All of these changes were commonly found in controls and, in addition, six have previously been reported as polymorphisms (10,27). Together, these data suggested that the UCMD phenotype in this patient was caused by a mutation in the gene for a protein that interacts with collagen VI and is important in microfibril structure. One such candidate is the small leucine rich repeat proteoglycan biglycan. To determine whether a biglycan mutation was present in UCMD3 the seven coding exons of the *BGN* gene including the consensus splice sites were PCR amplified and directly sequenced. No mutations were found.

DISCUSSION

UCMD has long been considered a recessively inherited condition (18), and until recently all of the collagen VI mutations that had been characterized in this disorder were either homozygous or compound heterozygous recessive mutations in the *COL6A2* or *COL6A3* genes (21–25). In contrast, the milder disorder Bethlem myopathy shows clear dominant inheritance within families and is caused by heterozygous mutations in *COL6A1*, *COL6A2* or *COL6A3* (7,9,11–15). This collagen VI disease paradigm was challenged by the identification of a *de novo* heterozygous *COL6A1* mutation in a patient with classical severe UCMD (27). Our work now demonstrates that three out of a group of five UCMD patients have heterozygous dominant mutations and indicates that rather than being a rare cause of UCMD (one out of 10 patients), dominant mutations are common in UCMD, now accounting for four of the 14 published cases. The incidence of recessive UCMD may have been overestimated because the parents of four of the 10 previously reported cases were consanguinous (21,25). This finding will have a major impact on the genetic counseling advice that parents of UCMD patients receive, and mutation detection is clearly critical for accurate advice to be provided.

The dominant UCMD mutations were all heterozygous in-frame deletions in the triple helical domain of collagen VI. While the mutations were in different chains, they were all located close to the N-terminal region of the triple helix, between amino acids 13 and 63 of the 335–336 residue helical domain (Fig. 7A), and this explains their similar effect on collagen VI intracellular and extracellular assembly. These dominant UCMD mutations identify, for the first time, a protein domain important for collagen VI tetramer formation, and provide new insights into the interacting protein domains that are involved in intracellular and extracellular collagen VI assembly. Interactions between the C-terminal globular domains of α1(VI), α2(VI) and α3(VI) lead to the formation of heterotrimeric monomers (16,33). Monomers then align in a staggered antiparallel manner with a 75 nm overlap in the triple helix to form dimers that are stabilized by disulfide bonds involving cysteine residues within the triple helix of one monomer and the C-terminal globular domain of the other (1) (Fig. 7B). Both α1(VI) and α2(VI) have a cysteine at amino acid 89 of the triple helix. Although it is not yet known which one of these cysteines forms the disulfide bridge that stabilizes the dimer, deletion of α1(VI) exon 14, which encodes amino acids 79–96 of the helix and includes cysteine 89, completely prevents dimer formation, indicating that the structure of the triple helix in this region is critical

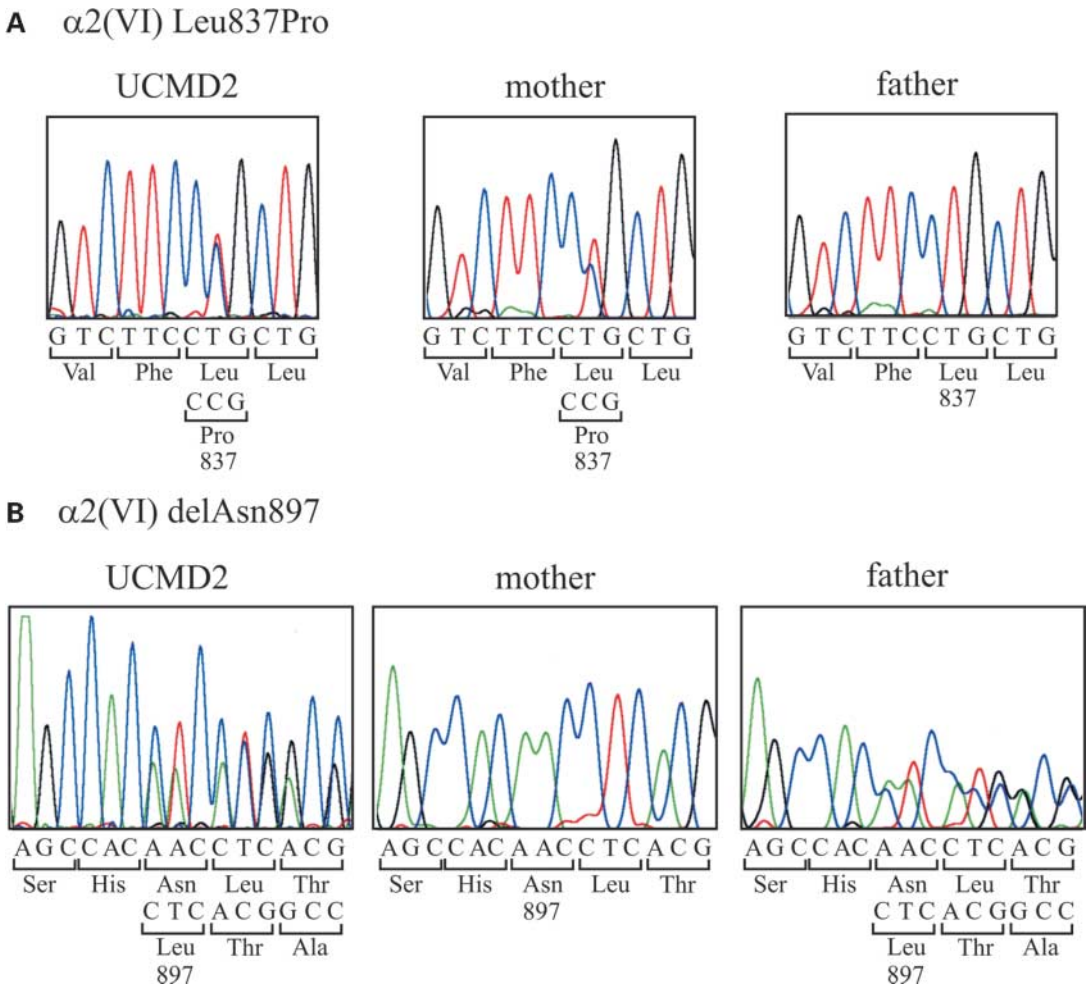

Figure 6. UCMD2 has recessive mutations in the α2(VI) chain. The entire coding regions of the α1(VI), α2(VI) and α3(VI) mRNAs were amplified by RT–PCR and directly sequenced. Two heterozygous mutations in the C-terminal globular domain of the α2(VI) chain were identified. **(A)** UCMD2 is heterozygous for a c.2510T>C mutation that changes amino acid 837 from a Leu to a Pro. This mutation was inherited from the unaffected mother. **(B)** UCMD2 is also heterozygous for a 3 bp deletion, c.2699delAAC that leads to the deletion of Asn897 from the α2(VI) chain. This mutation was inherited from the unaffected father.

for assembly of dimers (13,27). Recent *in vitro* assembly experiments suggest that amino acids 106–113 of the α2(VI) helix may play a role in dimer formation by interacting with the α2(VI) C2 subdomain; however, this has yet to be confirmed in cells expressing all three collagen VI subunits (34). Our finding that dimers are able to form from monomers lacking amino acids 55–63 of the α1(VI) helical domain, 13–39 of the α2(VI) helical region or 16–33 of the α3(VI) helix, further delineates the region involved in dimer formation; triple helical amino acids 13–63 are not required, 79–96 are critical and 106–113 may also be important. This proposal is supported by the finding that dimers can form from monomers containing α1(VI) chains in which amino acids 13–45 of the triple helical region are deleted (27).

Collagen VI tetramers are generated by the parallel alignment of two dimers in register. Electron microscopy shows that the major, if not exclusive, contact regions are located in the outer 30 nm segments of the triple helix (35). In the tetramer, these regions cross over in a scissor-like fashion, and are linked by a disulfide bridge between the cystseines at amino acid 50 of the α3(VI) helical domain. Surprisingly, glycine substitutions at amino acid 49 of the α1(VI) and α3(VI) helix, which interrupt the repeating Gly-X-Y sequence and are likely to perturb the structure of the helix in this region, do not affect assembly of disulfide bonded tetramers (16). Disturbing the structure of the helix just C- or N-terminal to α3(VI) Cys50 by the incorporation of chains with in-frame deletions does, however, impair tetramer formation. This suggests that a large portion of the N-terminal region of the triple helix that does not overlap in the dimer is important for efficient tetramer assembly.

These biosynthetic and assembly studies also allow us to understand why these dominant mutations result in the severe UCMD phenotype rather than the milder disorder Bethlem myopathy. Initial association of the chains to form α1(VI)/α2(VI)/α3(VI) heterotrimeric monomers results in two populations of monomers, one containing the normal chain and one containing the mutant (Fig. 7B). Mutant monomers are able to form dimers and this would be expected to produce three populations of dimers. One population,

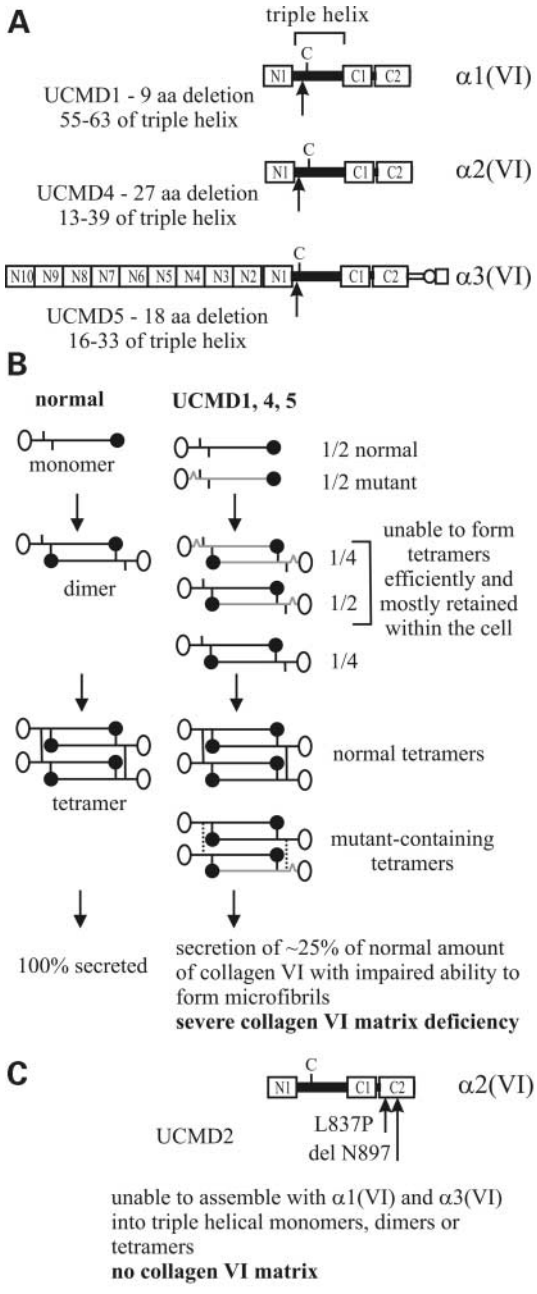

Figure 7. Schematic diagram showing the UCMD mutations and their effects on collagen VI assembly. **(A)** UCMD1, 4 and 5 have dominant heterozygous deletions (*arrows*) in the α1(VI), α2(VI) and α3(VI) chains, respectively. The mutations are all located towards the N-terminal end of the 335–336 amino acid triple helical domain (black box). The cysteine residues (C) at amino acid 89 of the α1(VI) and α2(VI) triple helical domain, and at amino acid 50 of the α3(VI) triple helix are indicated, and the N- and C-terminal subdomains that have homology to von Willebrand factor type A domains are labeled. **(B)** The normal collagen VI intracellular assembly steps are shown on the left. A collagen VI monomer forms when one α1(VI), one α2(VI) and one α3(VI) chain associate at the C-terminal region (black circles) and fold into a triple helix (black line). The critical triple helical cysteine residues are indicated by vertical lines. Dimers are formed by the staggered antiparallel association of monomers and are stabilized by a disulfide bond involving either the α1(VI) or α2(VI) cysteine at residue 89 of the triple helix. The dimers then associate laterally into tetramers. During this process, the outer regions of the triple helix cross over in a scissor-like fashion and the tetramers are stabilized by disulfide bonds involving the cysteines at amino acid 50 of the α3(VI) triple helix. Tetramers are secreted and associate end-to-end to form microfibrils. In UCMD1, 4 and 5 (right) equal amounts of normal and mutant chains are produced, leading to the assembly of equal amounts of normal and mutant (gray) monomers. The α1(VI) and α2(VI) cysteines that are critical for dimer formation are present in both normal and mutant monomers and so dimers with any combination of monomers are able to form. Only one-fourth of all dimers will contain two normal monomers and the remaining three-fourth of the dimers will contain either one or two mutant monomers. Mutant-containing dimers are unable to form tetramers efficiently, presumably because the structure of the N-terminal end of the triple helix is abnormal and interactions between these regions are critical for tetramer formation. Many of these mutant dimers are retained within the cell leading to reduced collagen VI secretion. The normal dimers can assemble into tetramers that are secreted. Some normal–mutant dimer assembly can also occur since the secreted tetramers are not able to form microfibrils as efficiently as in controls. This impaired intracellular assembly, reduced secretion and compromised end-to-end association of tetramers leads to a severe collagen VI matrix deficiency. **(C)** UCMD2 has compound heterozygous α2(VI) mutations, L837P and delN897, that are both in the C-terminal C2 subdomain. The mutant α2(VI) chains are almost completely unable to assemble with normal α1(VI) and α3(VI) to form triple helical monomers, and so almost no collagen VI is secreted.

representing one-fourth of the dimers, is composed of two normal monomers that are able to form tetramers and are secreted. The remaining three-quacters of the dimers contain either one or two mutant monomers and their assembly into tetramers is impaired (Fig. 7B). The UCMD cells secrete reduced amounts of collagen VI and this indicates that a substantial portion of the mutant-containing molecules are degraded inside the cell. Some mutant-containing tetramers are secreted, however, and they have a reduced ability to associate end-to-end into microfibrils and so the effects of the mutation are amplified even further. In the microfibrils, the N-terminal domains of adjacent tetramers are predicted to overlap in a junctional complex, allowing multiple potential interactions with each other, with the C-terminal domains and with the N-terminal region of the triple helix of the adjacent tetramers (1,35). One region that is necessary for microfibril formation is the N-terminal N5 subdomain of the α3(VI) chain (36), although its interacting partner has not been identified. Reduced end-to-end association of tetramers in the UCMD patients with deletions in the N-terminal region of the triple helix demonstrates that this region of the helix is also important in the interactions leading to microfibril formation. These dominant UCMD mutations thus act at the level of tetramer and microfibril formation and because of this they exert a severe dominant negative effect on collagen VI structure and assembly and result in a dramatic reduction in the amount of extracellular collagen VI that accounts for the severe phenotype. In contrast, the Bethlem myopathy deletion of amino acids 79–96 of the α1(VI) triple helical region acts at the level of dimer formation (13,27). Both mutant and normal monomers are assembled, but the mutant monomers are unable to form dimers and are degraded within the cell. This results in a 50% reduction in the amount of collagen VI, but the protein that is produced is structurally normal and the phenotype relatively mild.

These studies also highlight the importance of screening cDNA for understanding and predicting the consequences of changes in genomic DNA. The most common consequence of a mutation in the highly conserved 5′ GT and 3′ AG

splice site motifs is exon skipping (37), and this was the case for the 5′ GT to AT splice site mutations that were identified in UCMD1 and 5. However, splice site mutations do not always result in single exon skipping and other outcomes include activation of cryptic splice sites, creation of a pseudo-exon within an intron, intron retention and skipping of multiple exons (37,38). Predicting the strength of splice sites and the outcome of splice site mutations is not always straightforward and the *COL6A2* genomic deletion in UCMD4 emphasizes this. The deletion brings together sequences from intron 5 and exon 7 and provides a potential 3′ AG consensus splice site (Fig. 5). A polypyrimidine tract is usually present immediately upstream of 3′ splice sites (32). However, the new intron 5 3′ splice site does not have a pyrimidine-rich sequence as only eight out of the 20 most 3′ bases are pyrimidines, and as a result it has a low MaxENT splice site strength score that predicts it would not function as a splice site. In the absence of biological data, this genomic deletion would have been expected to result in the deletion of exon 6 and exon 7 sequences from the mRNA. The RT–PCR data clearly demonstrates that this is not the case and that the new low-scoring 3′ splice site is used, leading to inclusion of the remaining 27 bases of exon 7 in the mRNA.

Only one of our five patients, UCMD2, had recessive collagen VI mutations. Both mutations, L837P and delN897, were in the C-terminal C2 subdomain of the α2(VI) chain (Fig. 7C) and are the first two C2 subdomain mutations to be characterized. Almost no collagen VI was assembled and secreted by UCMD2 fibroblasts suggesting that the mutations prevented the initial chain association event. There is mounting evidence that the collagen VI C-terminal globular domains are critical for chain association. The C1 subdomain of each chain contains a putative α-helical coiled-coil oligomerization domain (39). These heptad repeat motifs have been shown to drive trimerization in transmembrane collagens (40,41), and in a reporter molecule containing a collagen-like sequence that does not spontaneously trimerize (39). The best experimental evidence for C-terminal chain association in collagen VI comes from analysis of naturally occurring and introduced triple helical glycine mutations. A glycine substitution towards the C-terminal region of the α3(VI) triple helix severely impairs association of the three chains and folding of the triple helix while similar mutations towards the N-terminal region of the triple helix do not affect assembly (16). One possibility is that in addition to sequences in the helix and the C1 subdomain, the C2 subdomain also contains sequence motifs that are important for chain association and the UCMD2 mutations disrupt these sequences and prevent the interactions that are necessary for assembly. This seems unlikely since constructs of the three collagen VI chains that contained just the C1 subdomain at the C-terminal region formed triple-helical monomers in *in vitro* transcription/translation experiments (33). A more plausible explanation is that the mutations cause the C2 subdomain to misfold, these misfolded chains are recognized by endoplasmic reticulum quality control mechanisms (42,43), are rapidly degraded and are therefore not available for assembly. Alignment of the protein sequence of the α2(VI) C2 subdomain with the von Willebrand factor A3-domain whose crystal structure has been determined (44) indicates that α2(VI) L837 is in the βA strand, one of the six β-strands that form the central β-sheet of the A domain. Proline residues are disfavored in β-sheets as they introduce a turn into the protein backbone (45,46), and this suggests that the L837P mutation is likely to destabilize the βA-strand and result in misfolding of the C2 subdomain. The deleted residue, α2(VI) N897, is within the consensus sequence for N-linked oligosaccharide addition, NLT. While it is not known if this glycosylation site is normally utilized, N-linked oligosaccharides are commonly important for correct protein structure and their removal can result in misfolding and intracellular degradation (47). The absence of collagen VI triple helical monomers indicates that these mutant chains do not take part in protein assembly and so they do not have a dominant negative effect on collagen VI assembly or structure. This accounts for the lack of a disease phenotype in the parents of UCMD2 who each carry one of the mutations.

Collagen VI microfibrils in the medium of UCMD3 cultures formed unusual large aggregates that were distinctly different from the individual microfibrils seen in controls and the other UCMD patients. This suggested that the collagen VI was structurally abnormal; however, we were unable to find a collagen VI mutation in UCMD3, even though the entire coding regions of the three collagen VI mRNAs, were sequenced. UCMD3 also produced normal levels of α1(VI), α2(VI) and α3(VI) mRNAs, indicating that there were no underlying premature stop codon mutations or mutations that prevented transcription of one of the collagen VI genes. The collagen VI genes have previously been excluded as the cause of UCMD in three families (19). A muscle biopsy was available from one of these patients and showed normal collagen VI staining (19), reminiscent of the normal levels of collagen VI staining in the UCMD3 fibroblast extracellular matrix. Aggregation of the collagen VI microfibrils in UCMD3 points to proteins that interact with collagen VI and are important in microfibril structure as the most obvious candidate disease genes in this patient. One such candidate was the small leucine rich repeat proteoglycan, biglycan. Biglycan binds close to the N-terminal region of the collagen VI triple helix (48) and also interacts with the critical skeletal muscle protein α-dystroglycan (49), thus potentially forming a bridge between α-dystroglycan and collagen VI. In addition, the biglycan null mouse has a muscular dystrophy phenotype (50), further implicating this molecule as a candidate disease gene in human muscular dystrophies. However, we did not find a biglycan mutation in UCMD3. It is thus likely that the UCMD phenotype in this patient is caused by a mutation in another, as yet unidentified gene.

MATERIALS AND METHODS

The patients

Five patients with a diagnosis of UCMD (UCMD1, 2, 3, 4 and 5) and their unaffected parents were studied. UCMD1, 2, 3 and 4 were from Belgium and UCMD5 from Australia. Dermal fibroblast cultures were established from skin biopsies of the patients and were grown in Dulbecco's modified Eagle's medium containing 10% fetal bovine serum (Life Technologies) in 5% CO_2 at 37°C as previously described (51). Genomic DNA was extracted from peripheral blood samples obtained from the parents.

RNA extraction and northern blot

Total RNA was isolated from confluent fibroblasts using RNeasy® (Qiagen). Total RNA (5 μg) was separated under denaturing conditions on a 1% agarose gel and transferred to nitrocellulose (52). The filter was hybridized simultaneously to [α-^{32}P]dCTP-labeled α1(VI), α2(VI) and α3(VI) cDNA probes [P18, P1 and P24 (3)], washed, and specific hybridization visualized by autoradiography.

Immunostaining of fibroblasts

Human fibroblasts were grown to confluence in four-well chamber glass slides (Nunc) and then supplemented daily for 2 days with 0.25 mM sodium ascorbate. To visualize collagen VI that had been deposited into the extracellular matrix, cell layers were washed with cold PBS then incubated with the collagen VI antibody 3C4 (53) for 1 h at 4°C. Bound antibody was detected using AlexaFluor® 488 goat anti-mouse IgG (Molecular Probes), cell nuclei were stained with 0.2 μg/ml 4,6-diamidino-2-phenylindole (DAPI) and the cell layers were then fixed with 4% paraformaldehyde for 15 min. Slides were mounted in FluorSave™reagent (Calbiochem) and then viewed and photographed using a Zeiss fluorescence microscope.

Immunostaining of muscle biopsy

Frozen sections (8 μm) were cut from patient muscle biopsies using a CM1900 Cryostat (Leica), and were mounted onto Superfrost® Plus slides (Menzel-Glaser). The sections were blocked with 2% (w/v) bovine serum albumin (BSA) in PBS for 15 min at room temperature, and then incubated at 4°C overnight with a primary antibody solution containing rabbit anti-collagen VI antibody (70-XR95, Fitzgerald Industries International, 1 : 20 000 dilution) and rat anti-perlecan antibody (clone A7L6, Chemicon International, 1 : 80 000 dilution) in 2% BSA. Slides were washed with PBS (3 × 5 min) then incubated for 1 h at room temperature with a secondary antibody solution containing a 1:250 dilution of Cy™-3 conjugated AffiniPure goat anti-rabbit IgG (Jackson ImmunoResearch Laboratories) and a 1 : 200 dilution of AlexaFluor® 488 conjugated goat anti-mouse IgG (Molecular Probes) in 2% BSA. The sections were then washed with PBS (3 × 5 min) and coverslipped with Immumount mounting media (Thermo-Shandon). Images were obtained using an Olympus BX50F4 microscope at 40× magnification.

Collagen VI immunoblotting

Human fibroblasts were seeded at the same density in 10 cm^2 dishes then grown until 2 days post-confluency. Cultures were incubated for 18 h in 0.5 ml of serum-free medium containing 0.25 mM sodium ascorbate, then 20 μl aliquots of the medium were separated under non-reducing conditions on composite gels. Proteins were electrophoretically transferred to Immobilon™-P Transfer Membrane (Millipore) and collagen VI detected with a polyclonal antibody (70-XR95, Fitzgerald Industries International) that recognizes all three collagen VI chains (9), peroxidase-conjugated swine anti-rabbit immunoglobulins (DAKO) and an enhanced chemiluminescence kit (ECL, Amersham Pharmacia Biotech).

Collagen VI biosynthetic labeling and analysis

Primary skin fibroblasts were grown to confluence in 10 cm^2 dishes, incubated overnight in the presence of 0.25 mM sodium ascorbate, and then biosynthetically labeled for 18 h with 100 μCi/ml [^{35}S]methionine (Tran^{35}S-label 1032 Ci/mmol, ICN Pharmaceuticals, Inc.) in 750 μl of methionine-free and serum-free Dulbecco's modified Eagle's medium containing 0.25 mM sodium ascorbate. The medium was removed to a sterile tube, and protease inhibitors were added to the following final concentrations: 1 mM 4-(2-aminoethyl)-benzenesulfonyl fluoride hydrochloride, 20 mM *N*-ethylmaleimide, and 5 mM EDTA. The cell layer was solubilized in 50 mM Tris/HCl, pH 7.5, containing 5 mM EDTA, 150 mM NaCl, 1% Nonidet P-40, 1 mM 4-(2-aminoethyl)-benzenesulfonyl fluoride hydrochloride, and 20 mM *N*-ethylmaleimide. Cell lysates and medium samples were clarified by centrifugation and then collagen VI was immunoprecipitated overnight at 4°C using an antibody raised in rabbits to the recombinant α3(VI) N1 subdomain, and 100 μl of 20% protein A-Separose (Amersham Biosciences). The protein A-sepharose beads were washed twice with NET buffer (50 mM Tris–HCl, pH 7.5, 150 mM NaCl, 5 mM EDTA, 0.1% Nonidet P-40) and then once with 10 mM Tris–HCl, pH 7.5, 0.1% Nonidet P-40 for 30 min each. Immunoprecipitated collagen VI was eluted into gel loading buffer at 65°C for 15 min and analyzed following reduction with 25 mM dithiothreitol by SDS–PAGE on 3–8% (w/v) gradient polyacrylamide gels. Collagen VI triple helical monomers, dimers and tetramers were analyzed on 2.4% (w/v) acrylamide, 0.5% (w/v) agarose composite gels under non-reducing conditions as described previously (13,15,16). Radioactively labeled proteins were detected by fluorography (51) or autoradiography.

Electron microscopy

Confluent human fibroblasts in 10 cm^2 dishes were incubated for 18 h in 1 ml of serum-free medium containing 0.25 mM sodium ascorbate. The medium was collected; the protease inhibitors described earlier were added, and sodium azide was included at a final concentration of 0.1% (w/v). Culture medium was clarified by centrifugation, adsorbed onto carbon-coated grids for 1 min, washed with water and stained with 0.75% uranyl formate. The grids were rendered hydrophilic by glow discharge in air, and samples were observed in a JEOL 1200 EX electron microscope operated at 60 kV accelerating voltage.

Mutational analysis by RT–PCR, genomic PCR and DNA sequencing

Total RNA was reverse transcribed using MuLV reverse transcriptase and an oligo(dT) primer for 1 h at 42°C (GeneAmp®

RNA PCR Kit, Applied Biosystems). The resulting cDNA was used as a template for PCR amplification of the entire coding regions of the α1(VI) and α2(VI) mRNAs (nine and 10 primer pairs, respectively) and the region of the α3(VI) mRNA coding for protein domains N3–C5 (15 primer pairs). Exons 1–9 of *COL6A3*, coding for the α3(VI) signal peptide and protein domains N10–N4 were PCR amplified using genomic DNA as a template. Touchdown PCR conditions were 95°C for 5 min, 14 cycles of 95°C for 20 s, 20 s annealing at 63–56°C (decreasing by 0.5°C each cycle), and 72°C for 45 s, then 16 cycles of 95°C for 20 s, 56°C for 20 s, and 72°C for 45 s, followed by a final extension at 72°C for 5 min. PCR products were sequenced using the BigDye® Terminator v3.1 Cycle Sequencing Kit (Applied Biosystems) and the primers used for PCR. Sequencing products were analyzed on a 3730xl DNA Analyzer (Applied Biosystems).

To characterize the genomic mutation in UCMD1 genomic DNA from the patient and parents was PCR amplified using primers within *COL6A1* intron 10 (5′-TTGCACAG-CACTAACAAGCC-3′) and *COL6A1* intron 13 (5′-TCACCTTCACACTGTCCACC-3′). The intron 13 primer was used for sequencing.

To determine whether the parents of UCMD2 carried the *COL6A2* mutations genomic DNA was PCR amplified using primers within intron 27 (5′-AATGGAAGGGCACAGGTGC G-3′) and the 3′untranslated region of exon 28 (5′-CTTAGC ACCATGGACGGGGT-3′) and the GC-RICH PCR System (Roche Applied Science). The intron 27 primer was used for sequencing.

The genomic DNA deletion in UCMD4 was characterized by PCR amplification with a primer located in *COL6A2* intron 4 (5′CAGGGCATTTCAGCATCTCC-3′) and a primer spanning the *COL6A2* exon 8/intron 8 boundary (5′-AAGAGCCT CACCTTCTCTCC-3′). The 1156 bp product containing the deletion was sequenced using an internal primer within intron 7 (5′-CAAACAGTCTGCGGAGGAGG-3′). To determine whether the mutation was present in the parents, genomic DNA was PCR amplified using a primer within *COL6A2* intron 5 (5′-GAAGGAACCTCTTTTGTGGC-3′) and a primer that spanned the exon7/intron 7 boundary (5′-AGGT CACTCACCTTGGGTCC-3′). This primer set was predicted to amplify a 1396 bp product from the normal allele and a 64 bp product from the mutant allele.

To characterize the mutation in UCMD5 genomic DNA from the patient and parents was PCR amplified using primers within *COL6A3* intron 15 (5′-GTGCTTTAACA GCTTGGTCC-3′) and intron 16 (5′-ATCTGATCCAGCAA CATCCC-3′). The intron 16 primer was used for sequencing.

Bioinformatic sequence analysis

To estimate the strength of the newly created *COL6A2* intron 5 3′ splice junction in UCMD4, the sequence was scored using the splice site prediction model of Yeo and Burge (32) and the software available at: http://genes.mit.edu/burgelab/maxent/Xmaxentscan_scoreseq_acc.html. This software takes into account large data sets of human splice sites and calculates a log-likelihood ratio (maximum entropy score, MaxENT) for a 23 base 3′splice site sequence. The maximum score for a 3′ splice site is 13.59 and the higher the score, the higher the probability that the sequence is a true splice site (31).

The SignalP 3.0 program available at http://www.cbs.dtu.dk/services/SignalP was used to predict whether the normal and alternative α3(VI) N-terminal sequences would function as signal peptides. A 55 amino acid sequence that included the signal peptide and the N-terminal region of the N10 subdomain was analyzed.

ACKNOWLEDGEMENTS

We would like to thank the patients and their parents for their involvement in this work. This work was supported by grants from the National Health and Medical Research Council of Australia.

REFERENCES

1. Timpl, R. and Chu, M.-L. (1994) Microfibrillar collagen type VI. In Yurchenco, P.D., Birk, D. and Mecham, R.P. (eds), *Extracellular Matrix Assembly and Structure.* Academic Press, Orlando, pp. 207–242.
2. Timpl, R. and Engel, J. (1987) Type VI collagen. In Mayne, R. and Burgeson, R.E. (eds), *Structure and Function of Collagen Types.* Academic Press, Orlando, pp. 105–143.
3. Chu, M.L., Conway, D., Pan, T.C., Baldwin, C., Mann, K., Deutzmann, R. and Timpl, R. (1988) Amino acid sequence of the triple-helical domain of human collagen type VI. *J. Biol. Chem.*, **263**, 18601–18606.
4. Chu, M.L., Pan, T.C., Conway, D., Saitta, B., Stokes, D., Kuo, H.J., Glanville, R.W., Timpl, R., Mann, K. and Deutzmann, R. (1990) The structure of type VI collagen. *Ann. NY Acad. Sci.*, **580**, 55–63.
5. Chu, M.L., Zhang, R.Z., Pan, T.C., Stokes, D., Conway, D., Kuo, H.J., Glanville, R., Mayer, U., Mann, K., Deutzmann, R. *et al.* (1990) Mosaic structure of globular domains in the human type VI collagen alpha 3 chain: similarity to von Willebrand factor, fibronectin, actin, salivary proteins and aprotinin type protease inhibitors. *EMBO J.*, **9**, 385–393.
6. Chu, M.-L., Pan, T., Conway, D., Kuo, H.-J., Glanville, R.W., Timpl, R., Mann, K. and Deutzmann, R. (1989) Sequence analysis of α1(VI) and α2(VI) chains of human type VI collagen reveals internal triplication of globular domains similar to the A domains of van Willebrand factor and two α2(VI) chain variants that differ in the carboxy terminus. *EMBO J.*, **8**, 1939–1946.
7. Jobsis, G.J., Keizers, H., Vreijling, J.P., de Visser, M., Speer, M.C., Wolterman, R.A., Baas, F. and Bolhuis, P.A. (1996) Type VI collagen mutations in Bethlem myopathy, an autosomal dominant myopathy with contractures. *Nat. Genet.*, **14**, 113–115.
8. Bethlem, J. and van Wijngaarden, G.K. (1976) Benign myopathy, with autosomal dominant inheritance: a report on three pedigrees. *Brain*, **99**, 91–100.
9. Scacheri, P.C., Gillanders, E.M., Subramony, S.H., Vedanarayanan, V., Crowe, C.A., Thakore, N., Bingler, M. and Hoffman, E.P. (2002) Novel mutations in collagen VI genes: expansion of the Bethlem myopathy phenotype. *Neurology*, **58**, 593–602.
10. Pan, T.-C., Zhang, R.-Z., Pericak-Vance, M.A., Tandan, R., Fries, T., Stajich, J.M., Viles, K., Vance, J.M., Chu, M.-L. and Speer, M.C. (1998) Missense mutation in a von Willebrand factor type A domain of the α3(VI) collagen gene (*COL6A3*) in a family with Bethlem myopathy. *Hum. Mol. Genet*, **7**, 807–812.
11. Pepe, G., Bertini, E., Giusti, B., Brunelli, T., Comeglio, P., Saitta, B., Merlini, L., Chu, M.-L., Federici, G. and Abbate, R. (1999) A novel de novo mutation in the triple helix of the *COL6A3* gene in a two-generation Italian family affected by Bethlem myopathy. A diagnostic approach in the mutations' screening of type VI collagen. *Neuromusc. Disord.*, **9**, 264–271.
12. Vanegas, O.C., Zhang, R.Z., Sabatelli, P., Lattanzi, G., Bencivenga, P., Giusti, B., Columbaro, M., Chu, M.L., Merlini, L. and Pepe, G. (2002) Novel *COL6A1* splicing mutation in a family affected by mild Bethlem myopathy. *Muscle Nerve*, **25**, 513–519.

13. Lamande, S.R., Shields, K.A., Kornberg, A.J., Shield, L.K. and Bateman, J.F. (1999) Bethlem myopathy and engineered collagen VI triple helical deletions prevent intracellular multimer assembly and protein secretion. *J. Biol.Chem.*, **274**, 21817–21822.
14. Pepe, G., Giusti, B., Bertini, E., Brunelli, T., Saitta, B., Comeglio, P., Bolognese, A., Merlini, L., Federici, G., Abbate, R. *et al.* (1999) A heterozygous splice site mutation in *COL6A1* leading to an in-frame deletion of the α1(VI) collagen chain in an Italian family affected by Bethlem myopathy. *Biochem. Biophys. Res. Commun.*, **258**, 802–807.
15. Lamande, S.R., Bateman, J.F., Hutchison, W., McKinlay Gardner, R.J., Bower, S.P., Byrne, E. and Dahl, H.H. (1998) Reduced collagen VI causes Bethlem myopathy: a heterozygous *COL6A1* nonsense mutation results in mRNA decay and functional haploinsufficiency. *Hum. Mol. Genet.*, **7**, 981–989.
16. Lamande, S.R., Morgelin, M., Selan, C., Jobsis, G.J., Baas, F. and Bateman, J.F. (2002) Kinked collagen VI tetramers and reduced microfibril formation as a result of Bethlem myopathy and introduced triple helical glycine mutations. *J. Biol. Chem.*, **277**, 1949–1956.
17. De Paillette, L., Aicardi, J. and Goutieres, F. (1989) Ullrich's congenital atonic sclerotic muscular dystrophy. A case report. *J. Neurol.*, **236**, 108–110.
18. Nonaka, I., Une, Y., Ishihara, T., Miyoshino, S., Nakashima, T. and Sugita, H. (1981) A clinical and histological study of Ullrich's disease (congenital atonic–sclerotic muscular dystrophy). *Neuropediatrics*, **12**, 197–208.
19. Mercuri, E., Yuva, Y., Brown, S.C., Brockington, M., Kinali, M., Jungbluth, H., Feng, L., Sewry, C.A. and Muntoni, F. (2002) Collagen VI involvement in Ullrich syndrome: a clinical, genetic, and immunohistochemical study. *Neurology*, **58**, 1354–1359.
20. Voit, T. (1998) Congenital muscular dystrophies: 1997 update. *Brain Dev.*, **20**, 65–74.
21. Vanegas, O.C., Bertini, E., Zhang, R.-Z., Petrini, S., Minosse, C., Sabatelli, P., Giusti, B., Chu, M.-L. and Pepe, G. (2001) Ullrich scleroatonic muscular dystrophy is caused by recessive mutations in collagen type VI. *Proc. Natl Acad. Sci. USA*, **98**, 7516–7521.
22. Ishikawa, H., Sugie, K., Murayama, K., Awaya, A., Suzuki, Y., Noguchi, S., Hayashi, Y.K., Nonaka, I. and Nishino, I. (2004) Ullrich disease due to deficiency of collagen VI in the sarcolemma. *Neurology*, **62**, 620–623.
23. Ishikawa, H., Sugie, K., Murayama, K., Ito, M., Minami, N., Nishino, I. and Nonaka, I. (2002) Ullrich disease: collagen VI deficiency: EM suggests a new basis for muscular weakness. *Neurology*, **59**, 920–923.
24. Higuchi, I., Shiraishi, T., Hashiguchi, T., Suehara, M., Niiyama, T., Nakagawa, M., Arimura, K., Maruyama, I. and Osame, M. (2001) Frameshift mutation in the collagen VI gene causes Ullrich's disease. *Ann. Neurol.*, **50**, 261–265.
25. Demir, E., Sabatelli, P., Allamand, V., Ferreiro, A., Moghadaszadeh, B., Makrelouf, M., Topaloglu, H., Echenne, B., Merlini, L. and Guicheney, P. (2002) Mutations in *COL6A3* cause severe and mild phenotypes of Ullrich congenital muscular dystrophy. *Am. J. Hum. Genet.*, **70**, 1446–1458.
26. Zhang, R.Z., Sabatelli, P., Pan, T.C., Squarzoni, S., Mattioli, E., Bertini, E., Pepe, G. and Chu, M.L. (2002) Effects on collagen VI mRNA stability and microfibrillar assembly of three *COL6A2* mutations in two families with Ullrich congenital muscular dystrophy. *J. Biol. Chem.*, **277**, 43557–43564.
27. Pan, T.C., Zhang, R.Z., Sudano, D.G., Marie, S.K., Bonnemann, C.G. and Chu, M.-L. (2003) New molecular mechanism for Ullrich congenital muscular dystrophy: a heterozygous in-frame deletion in the *COL6A1* gene causes a severe phenotype. *Am. J. Hum. Genet.*, **73**, 355–369.
28. Maquat, L.E. (2002) Nonsense-mediated mRNA decay. *Curr. Biol.*, **12**, R196–197.
29. Byers, P.H. (2002) Killing the messenger: new insights into nonsense-mediated mRNA decay. *J. Clin. Invest.*, **109**, 3–6.
30. Mankodi, A. and Ashizawa, T. (2003) Echo of silence: silent mutations, RNA splicing, and neuromuscular diseases. *Neurology*, **61**, 1330–1331.
31. Eng, L., Coutinho, G., Nahas, S., Yeo, G., Tanouye, R., Babaei, M., Dork, T., Burge, C. and Gatti, R.A. (2004) Nonclassical splicing mutations in the coding and noncoding regions of the *ATM* gene: maximum entropy estimates of splice junction strengths. *Hum. Mutat.*, **23**, 67–76.
32. Yeo, G. and Burge, C.B. (2004) Maximum entropy modeling of short sequence motifs with applications to RNA splicing signals. *J. Comp. Biol.*, **11**, 377–394.
33. Ball, S.G., Baldock, C., Kielty, C.M. and Shuttleworth, C.A. (2001) The role of the C1 and C2 a-domains in type VI collagen assembly. *J. Biol. Chem.*, **276**, 7422–7430.
34. Ball, S., Bella, J., Kielty, C. and Shuttleworth, A. (2003) Structural basis of type VI collagen dimer formation. *J. Biol. Chem.*, **278**, 15326–15332.
35. Furthmayr, H., Wiedemann, H., Timpl, R., Odermatt, E. and Engel, J. (1983) Electron-microscopical approach to a structural model of intima collagen. *Biochem. J.*, **211**, 303–311.
36. Fitzgerald, J., Morgelin, M., Selan, C., Wiberg, C., Keene, D.R., Lamande, S.R. and Bateman, J.F. (2001) The N-terminal N5 subdomain of the alpha 3(VI) chain is important for collagen VI microfibril formation. *J. Biol. Chem.*, **276**, 187–193.
37. Berget, S.M. (1995) Exon recognition in vertebrate splicing. *J. Biol. Chem.*, **270**, 2411–2414.
38. Takahara, K., Schwarze, U., Imamura, Y., Hoffman, G.G., Toriello, H., Smith, L.T., Byers, P.H. and Greenspan, D.S. (2002) Order of intron removal influences multiple splice outcomes, including a two-exon skip, in a *COL5A1* acceptor-site mutation that results in abnormal pro-alpha1(V) N-propeptides and Ehlers–Danlos syndrome type I. *Am. J. Hum. Genet.*, **71**, 451–465.
39. McAlinden, A., Smith, T.A., Sandell, L.J., Ficheux, D., Parry, D.A. and Hulmes, D.J. (2003) Alpha-helical coiled-coil oligomerization domains are almost ubiquitous in the collagen superfamily. *J. Biol. Chem.*, **278**, 42200–42207.
40. Latvanlehto, A., Snellman, A., Tu, H. and Pihlajaniemi, T. (2003) Type XIII collagen and some other transmembrane collagens contain two separate coiled-coil motifs, which may function as independent oligomerization domains. *J. Biol. Chem.*, **278**, 37590–37599.
41. Areida, S.K., Reinhardt, D.P., Muller, P.K., Fietzek, P.P., Kowitz, J., Marinkovich, M.P. and Notbohm, H. (2001) Properties of the collagen type XVII ectodomain. Evidence for N- to C-terminal triple helix folding. *J. Biol. Chem.*, **276**, 1594–1601.
42. Fitzgerald, J., Lamande, S.R. and Bateman, J.F. (1999) Proteasomal degradation of unassembled mutant type I collagen pro-alpha1(I) chains. *J. Biol. Chem.*, **274**, 27392–27398.
43. Lamande, S.R., Chessler, S.D., Golub, S.B., Byers, P.H., Chan, D., Cole, W.G., Sillence, D.O. and Bateman, J.F. (1995) Endoplasmic reticulum-mediated quality control of type I collagen production by cells from osteogenesis imperfecta patients with mutations in the pro alpha 1 (I) chain carboxyl-terminal propeptide which impair subunit assembly. *J. Biol. Chem.*, **270**, 8642–8649.
44. Bienkowska, J., Cruz, M., Atiemo, A., Handin, R. and Liddington, R. (1997) The von Willebrand factor A3 domain does not contain a metal ion-dependent adhesion site motif. *J. Biol. Chem.*, **272**, 25162–25167.
45. Chou, P.Y. and Fasman, G.D. (1978) Empirical predictions of protein conformation. *Annu. Rev. Biochem.*, **47**, 251–276.
46. Lifson, S. and Sander, C. (1979) Antiparallel and parallel beta-strands differ in amino acid residue preferences. *Nature*, **282**, 109–111.
47. Helenius, A. (1994) How N-linked oligosaccharides affect glycoprotein folding in the endoplasmic reticulum. *Mol. Biol. Cell.*, **5**, 253–265.
48. Wiberg, C., Hedbom, E., Khairullina, A., Lamande, S.R., Oldberg, A., Timpl, R., Morgelin, M. and Heinegard, D. (2001) Biglycan and decorin bind close to the n-terminal region of the collagen VI triple helix. *J. Biol. Chem.*, **276**, 18947–18952.
49. Bowe, M.A., Mendis, D.B. and Fallon, J.R. (2000) The small leucine-rich repeat proteoglycan biglycan binds to alpha-dystroglycan and is upregulated in dystrophic muscle. *J. Cell. Biol.*, **148**, 801–810.
50. Ameye, L. and Young, M.F. (2002) Mice deficient in small leucine-rich proteoglycans: novel in vivo models for osteoporosis, osteoarthritis, Ehlers–Danlos syndrome, muscular dystrophy, and corneal diseases. *Glycobiology*, **12**, 107R–116R.
51. Bateman, J.F., Mascara, T., Chan, D. and Cole, W.G. (1984) Abnormal type I collagen metabolism by cultured fibroblasts in lethal perinatal osteogenesis imperfecta. *Biochem. J.*, **217**, 103–115.
52. Sambrook, J., Fritsch, E.F. and Maniatis, T. (1989) *Molecular Cloning. A Laboratory Manual*, 2nd edn. Cold Spring Harbor Laboratory Press, Cold Spring Harbor.
53. Engvall, E., Hessle, H. and Klier, G. (1986) Molecular assembly, secretion, and matrix deposition of type VI collagen. *J. Cell Biol.*, **102**, 703–710.